

DUST PROPERTIES IN THE CRAB NEBULA

Using HAWC+ Polarisation

Jérémie Chastenet, Ilse De Looze, Brandon Hensley, Bert Vandenbroucke, Mike Barlow, Jeonghee Rho, Aravind P. Ravi, Haley L. Gomez, Anthony P. Jones, Florian Kirchschlager, Juan Macías-Pérez, Mikako Matsuura, Kate Pattle, Nicolas Ponthieu, Felix D. Priestley, Monica Relaño, Alessia Ritacco, Roger Wesson



DUST PROPERTIES IN THE CRAB NEBULA

A WORK IN PROGRESS
Using HAWC+ Polarisation



Jérémie Chastenet, Ilse De Looze, Brandon Hensley, Bert Vandenbroucke, Mike Barlow, Jeonghee Rho, Aravind P. Ravi, Haley L. Gomez, Anthony P. Jones, Florian Kirchschlager, Juan Macías-Pérez, Mikako Matsuura, Kate Pattle, Nicolas Ponthieu, Felix D. Priestley, Monica Relaño, Alessia Ritacco, Roger Wesson

DUST & SUPERNOVA REMNANTS

- Dust at low redshift
 - formed in the atmospheres of AGB stars; in the ejecta of SNe and SNRs; other kind of inflows and circulation
 - **but!** destroyed by strong winds of the very same SNRs that formed it; hot gas, cosmic rays, all kinds of collisions

→ grain growth must happen (but is hard to constrain)

→ overestimated destruction rates from SN shocks?

- **Also!** dust at high redshift → (significant?) production from SNRs

→ Really need to know how much SNRs produce and destroy

DUST MASSES IN SNRs (A VERY NON-EXHAUSTIVE LIST)

- Cassiopeia A: $0.02 - 1.1 M_{\odot}$ (Rho et al. 2008, Arendt et al. 2014, Barlow et al. 2010, Bevan et al. 2017, De Looze et al. 2017, Niculescu-Duvaz et al. 2021)
- G54.1+0.3: $0.06 - 1.1 M_{\odot}$ (Temim et al. 2010, Temim et al. 2017, Rho et al. 2018)
up to 3.38 in Priestley et al. (2020)
- SN1987A: $0.5 - 0.7 M_{\odot}$ (Matsuura et al. 2011)
- G11.2–0.3: $0.34 - 1.86 M_{\odot}$ (Chawner et al. 2020, Priestley et al. 2020)
- G21.5 – 0.9: $0.032 - 0.29 M_{\odot}$ (Chawner et al. 2020, Priestley et al. 2020)
- G29.7–0.3: $0.018 - 0.51 M_{\odot}$ (Chawner et al. 2020, Priestley et al. 2020)

DUST MASSES IN SNRs (A VERY NON-EXHAUSTIVE LIST)

- Cassiopeia A: $0.02 - 1.1 \text{ M}_\odot$ (Rho et al. 2008, Arendt et al. 2014, Barlow et al. 2010, Bevan et al. 2017, De Looze et al. 2017, Niculescu-Duvaz et al. 2021)
- G54.1+0.3: $0.06 - 1.1 \text{ M}_\odot$ (Temim et al. 2010, Temim et al. 2017, Rho et al. 2018)
up to **3.38** in Priestley et al. (2020)
- SN1987A: $0.5 - 0.7 \text{ M}_\odot$ (Matsuura et al. 2011)
- G11.2–0.3: $0.34 - 1.86 \text{ M}_\odot$ (Chawner et al. 2020, Priestley et al. 2020)
- G21.5 – 0.9: $0.032 - 0.29 \text{ M}_\odot$ (Chawner et al. 2020, Priestley et al. 2020)
- G29.7–0.3: $0.018 - 0.51 \text{ M}_\odot$ (Chawner et al. 2020, Priestley et al. 2020)

In the Crab:

- Gomez et al. (2012): 0.24 M_\odot of 28 K carbon grains
 0.11 M_\odot of 34 K silicate grains
 $0.14 + 0.08 \text{ M}_\odot$ of both
- Temim & Dwek (2013): 0.019 M_\odot of ~ 56 K carbon grains
- Owen & Barlow (2015): $0.18 - 0.27 \text{ M}_\odot$ of carbon grains
 $0.11 - 0.13 + 0.39 - 0.47 \text{ M}_\odot$ of both
- De Looze et al. (2019): $0.032 - 0.049 \text{ M}_\odot$ of 41 K carbon grains
similar masses for MgSiO_3
implausible masses for e.g. Fe or $\text{Mg}_{0.7}\text{SiO}_{2.7}$
- Priestley et al. (2020): 0.05 M_\odot ($0.026 - 0.076$) of carbon grains
 $0.076 - 0.218 \text{ M}_\odot$ of MgSiO_3

near-IR – radio fitting

radiative transfer

mid- – far-IR fitting

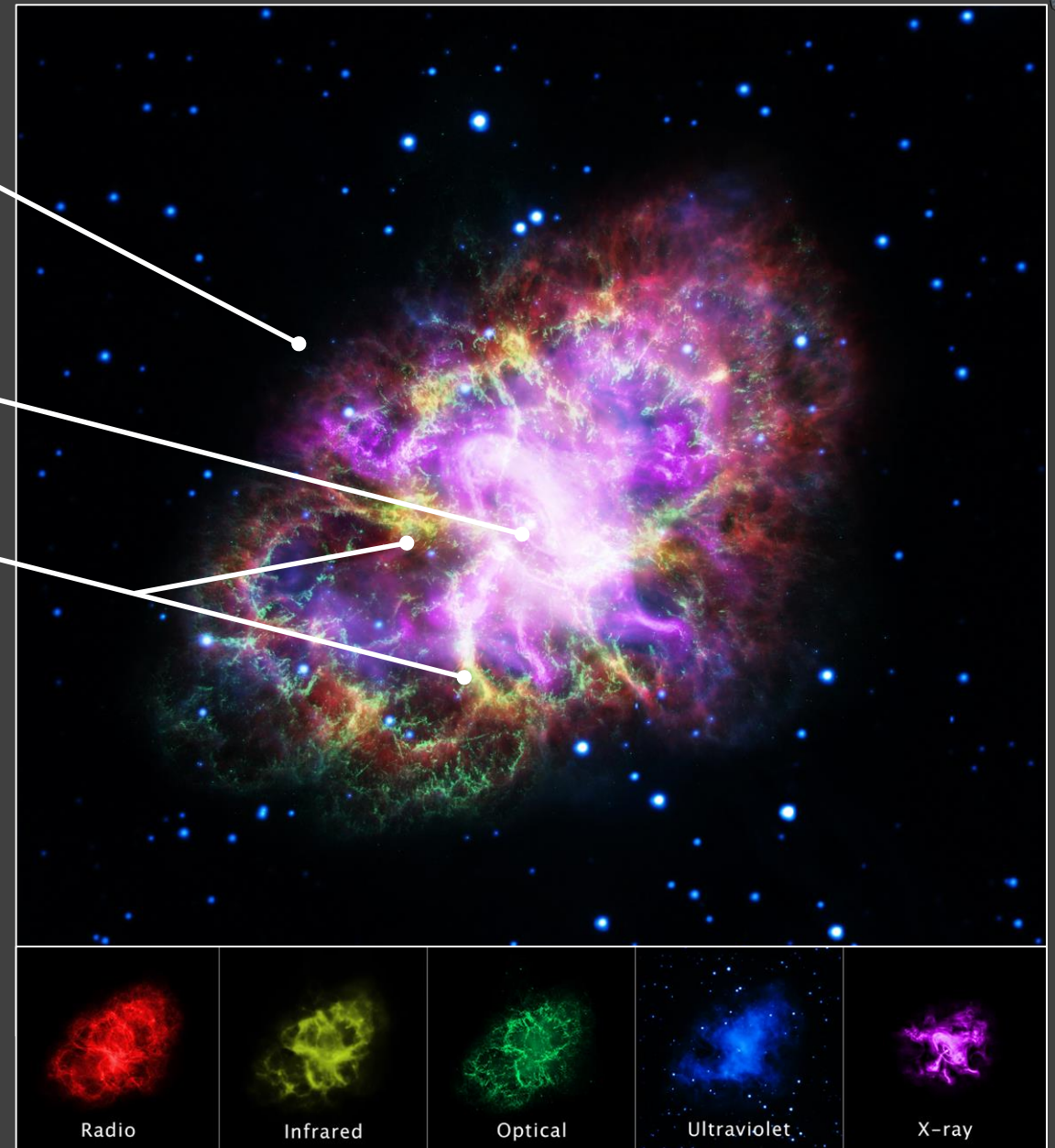
THE CRAB NEBULA



Exploded in 1054 AD*
2 kpc distance
Type II-P
 $8 - 11 M_{\odot}$ progenitor

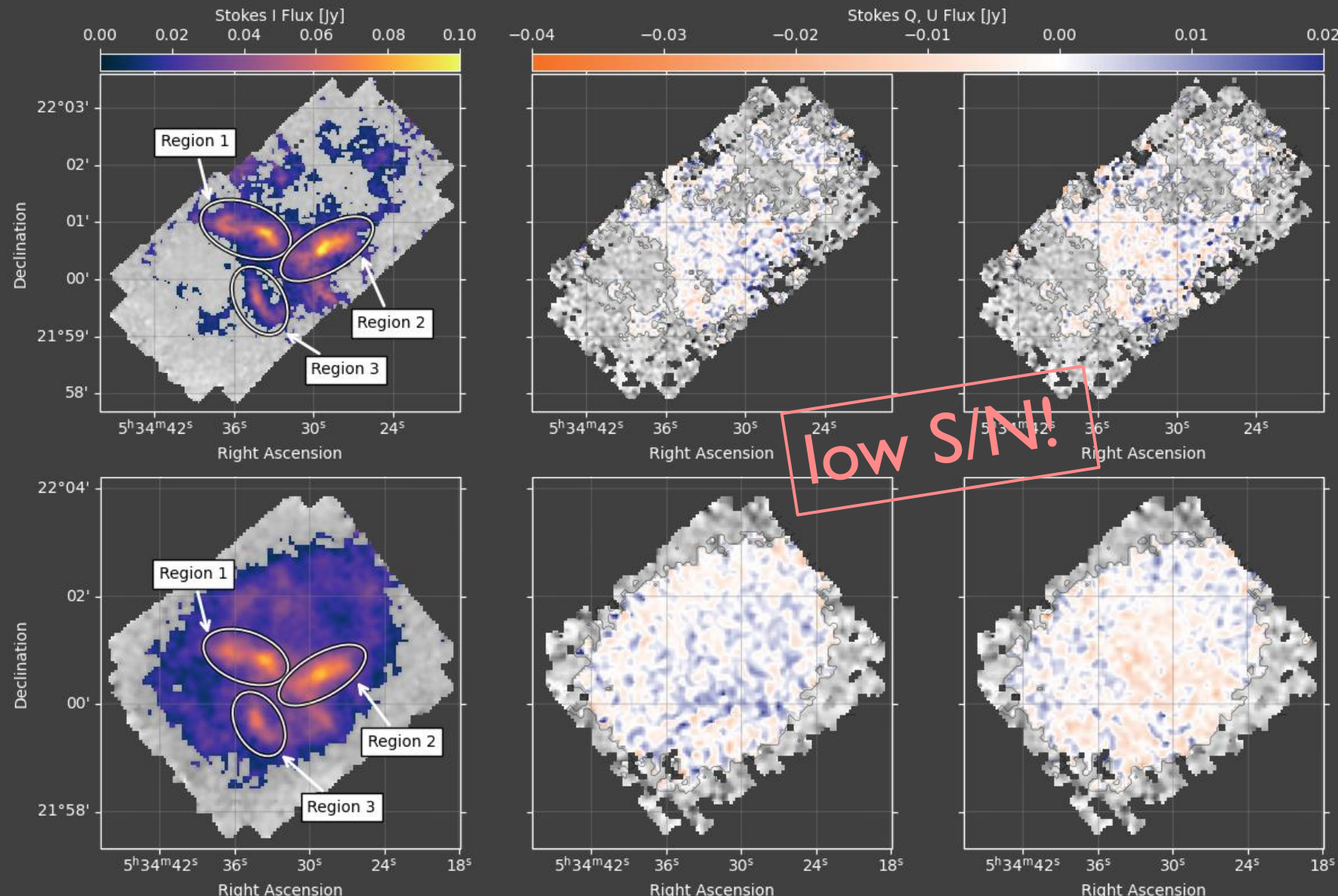
Pulsar Wind Nebula

85 – 90% He and lots of C, O, Ne, S, Ar

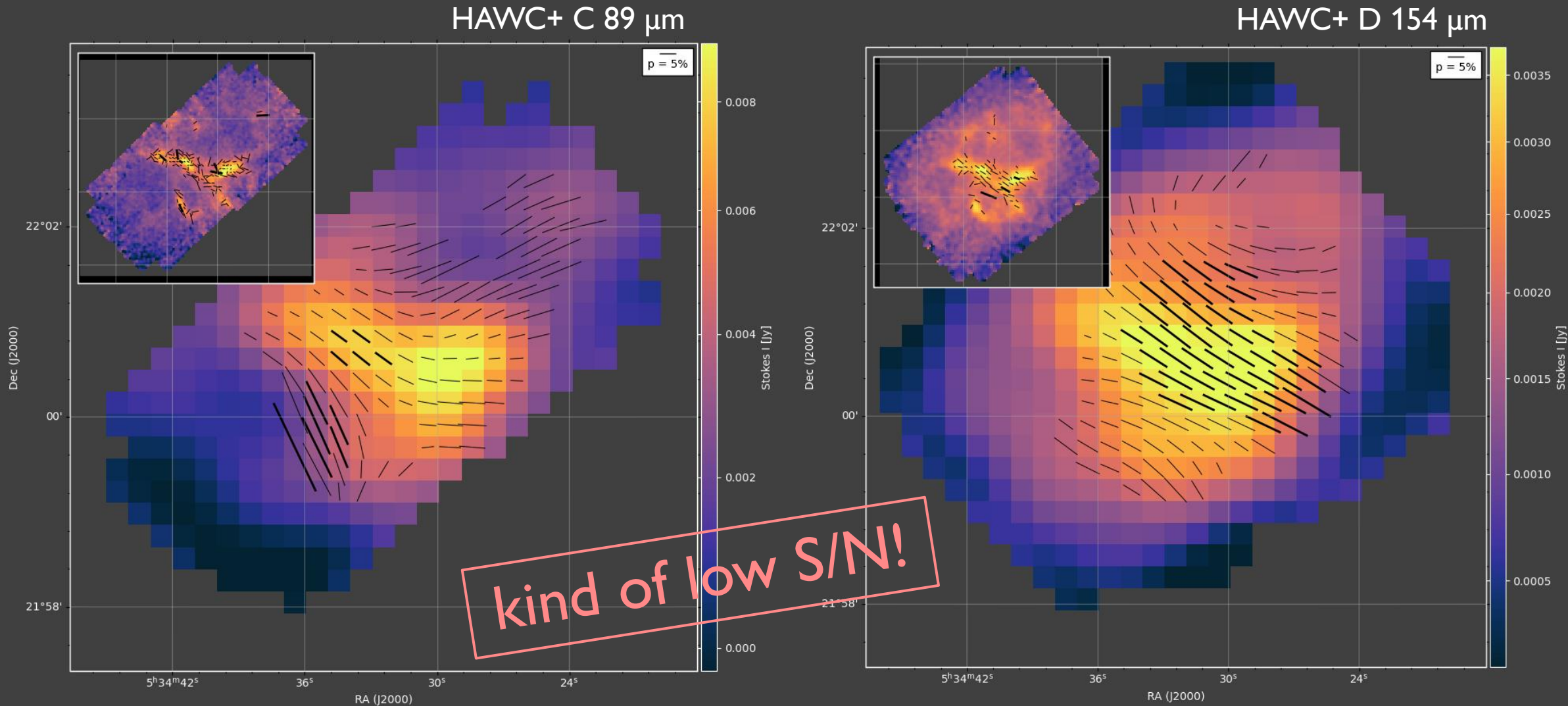


© NASA, ESA, G. Dubner (IAFE, CONICET-University of Buenos Aires) et al.; A. Loll et al.; T. Temim et al.; F. Seward et al.; VLA/NRAO/AUI/NSF; Chandra/CXC; Spitzer/JPL-Caltech; XMM-Newton/ESA; Hubble/STScI

THE POLARISED CRAB NEBULA WITH SOFIA

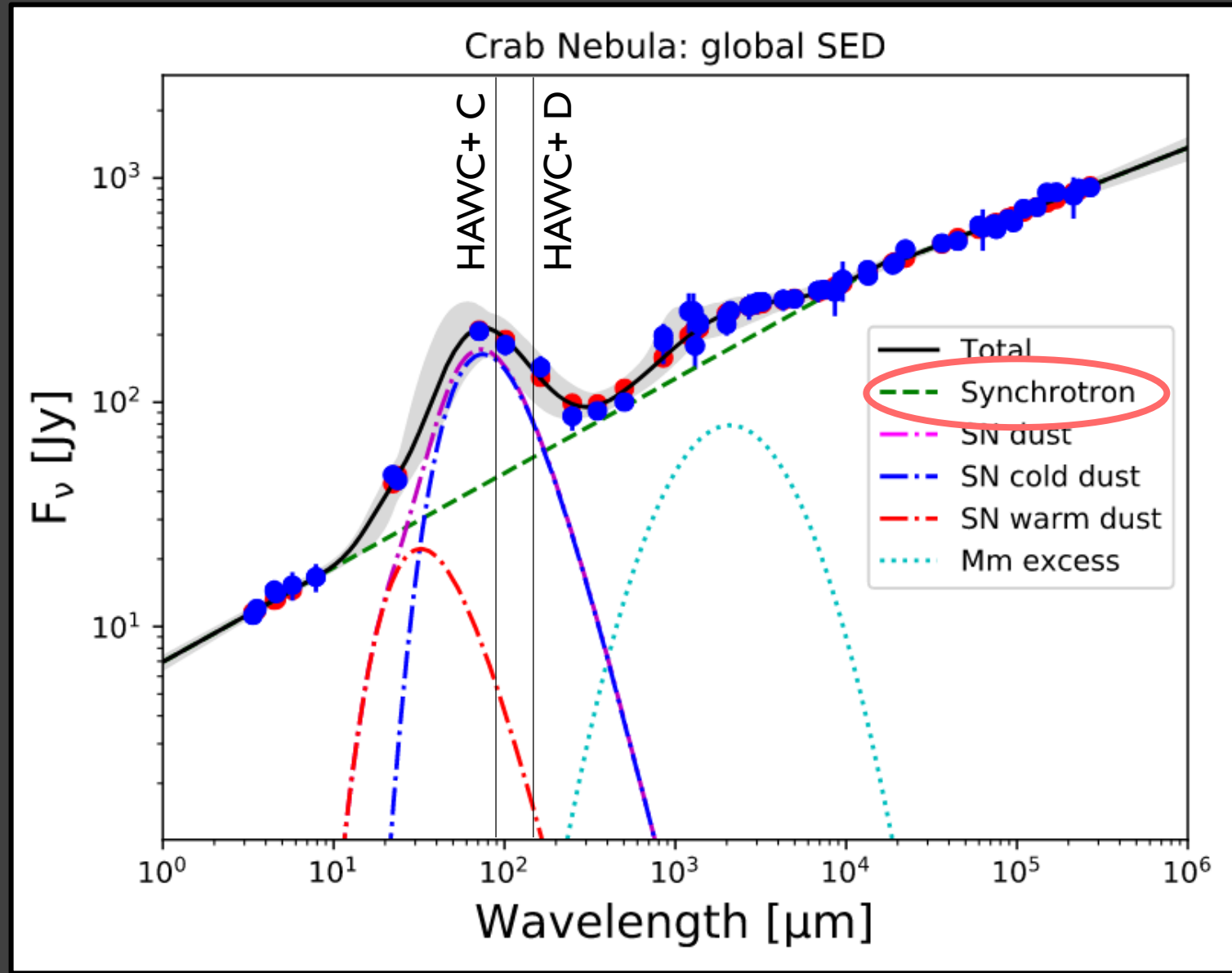


POLARISATION*



*using the Modified Asymptotic estimator from Plaszczynski et al. (2014)

POLARISATION, BUT!



De Looze et al. (2019)

SYNCHROTRON RADIATION REMOVAL

$$F_\nu = F_{\nu_0} \left(\frac{\nu}{\nu_0} \right)^{-\alpha_{\text{radio}}}$$

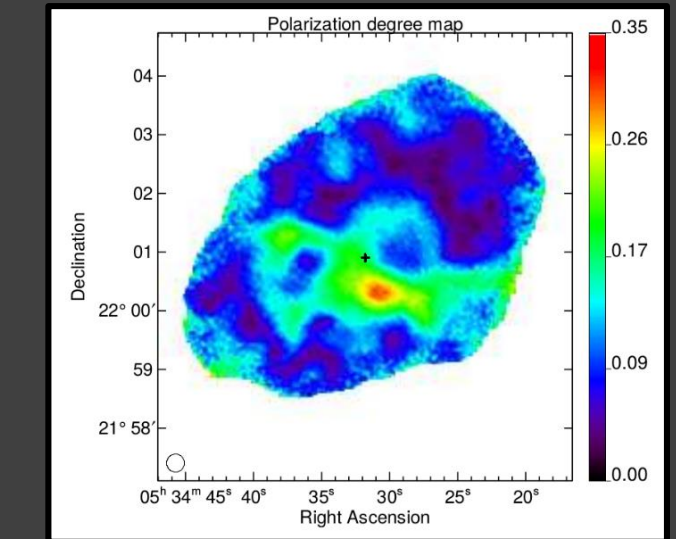
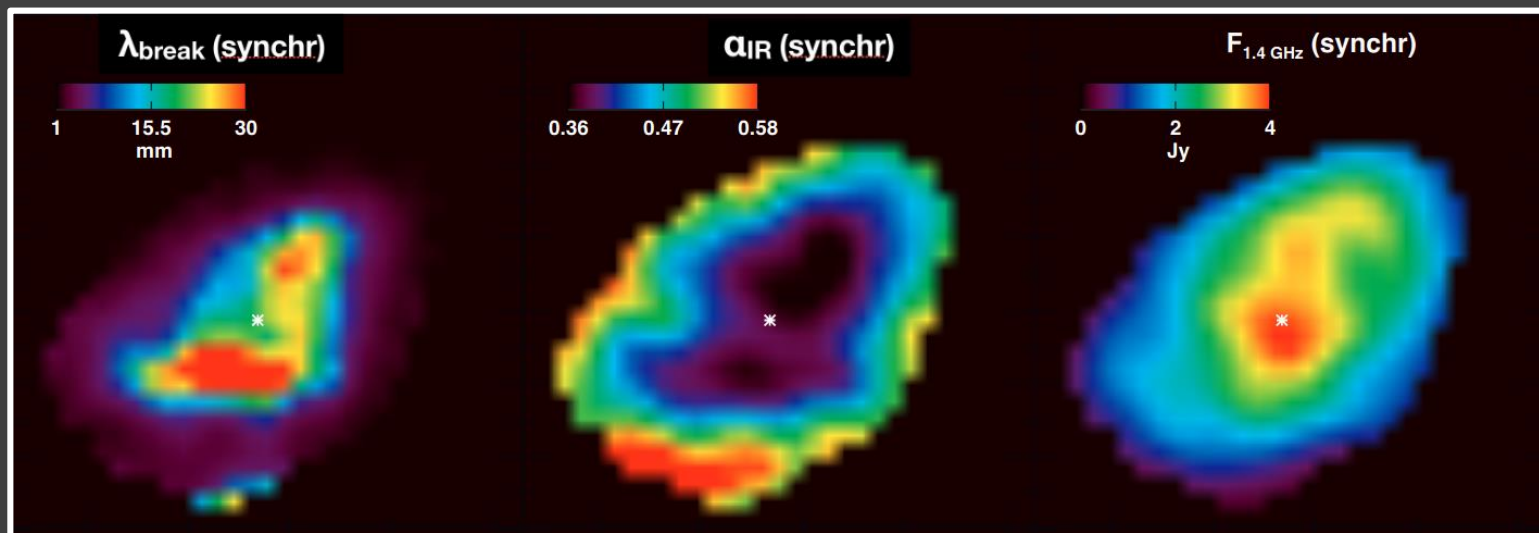
if $\lambda \geq \lambda_{\text{break}}$

$$F_{\nu_0} \left(\frac{\nu}{\nu_0} \right)^{-\alpha_{\text{IR}}} \times \left(\frac{\nu_{\text{break}}}{\nu_0} \right)^{-\alpha_{\text{radio}}} \left(\frac{\nu_{\text{break}}}{\nu_0} \right)^{\alpha_{\text{IR}}} \quad \text{if } \lambda < \lambda_{\text{break}}$$

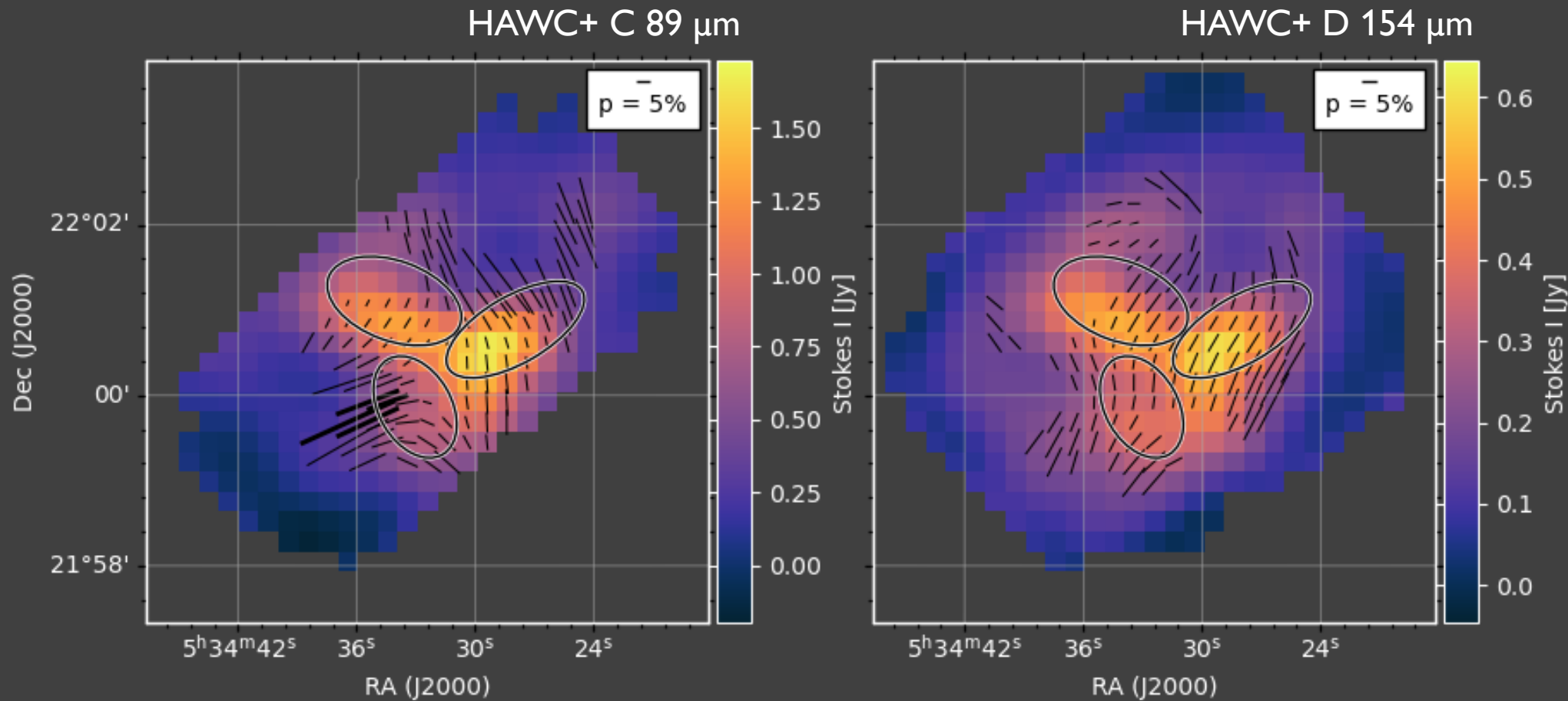
$p_{\text{radio}}, \theta_{\text{radio}}$



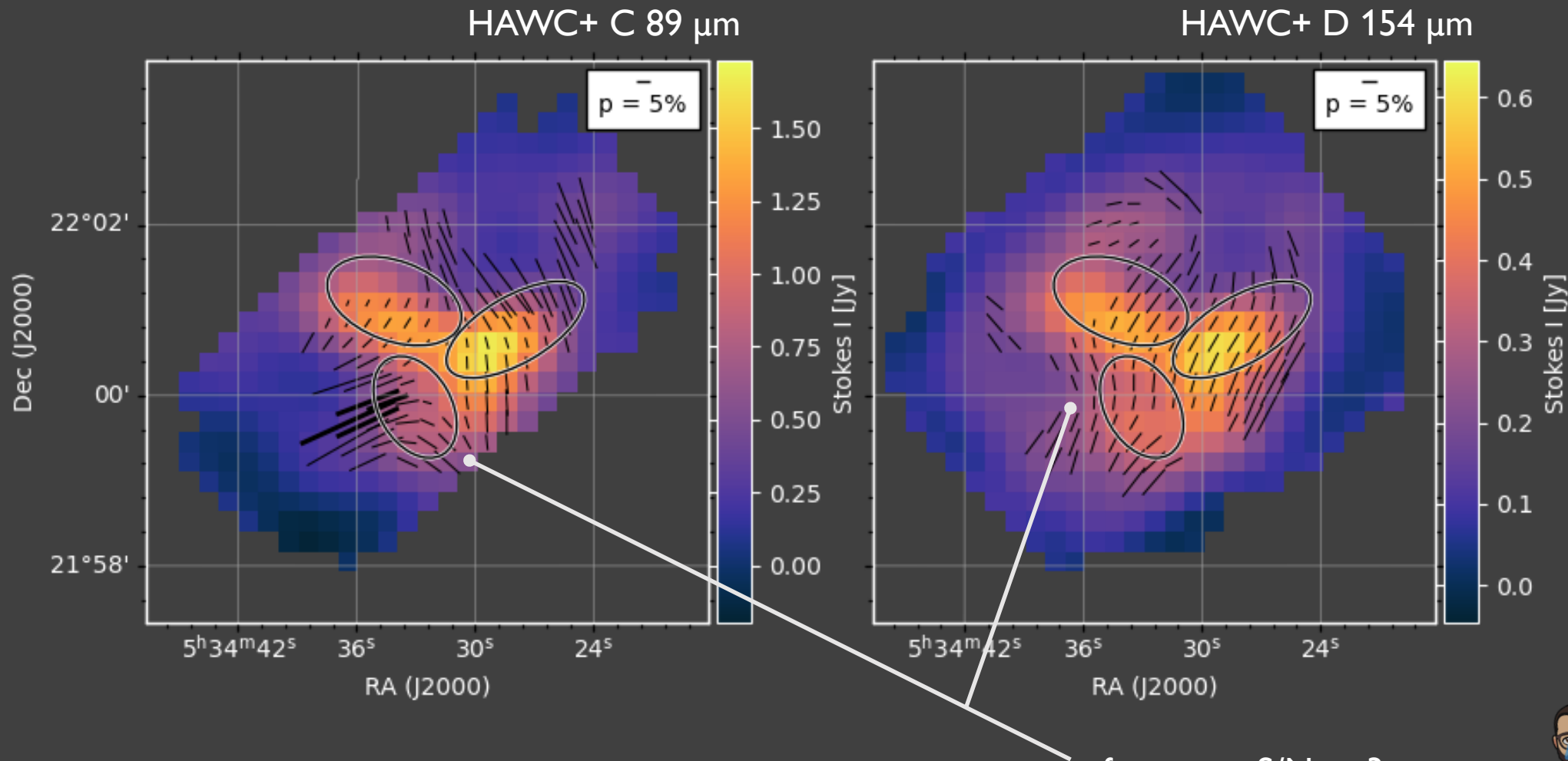
NIKA 150 GHz



SYNCHROTRON-FREE MAPS



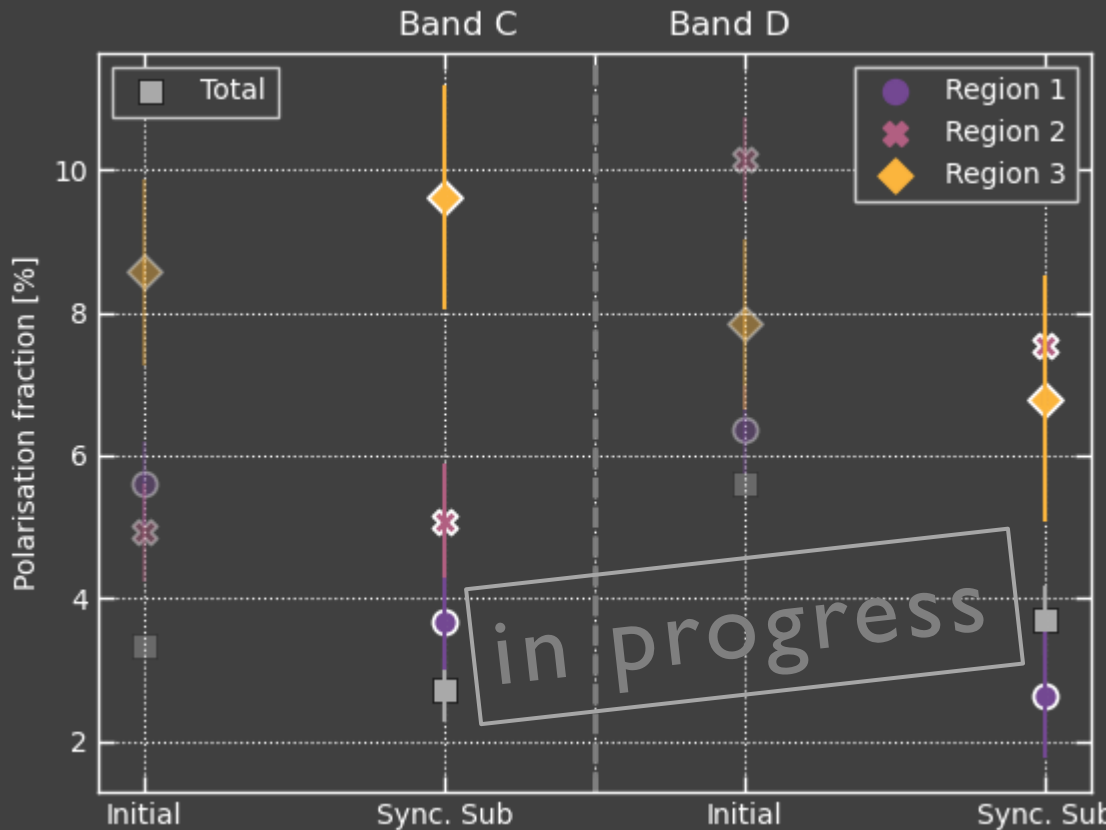
SYNCHROTRON-FREE MAPS



few to no $S/N_p > 3$ vectors
→ sum fluxes within regions



SYNCHROTRON-FREE POLARISATION



	HAWC+ C 89 μm	HAWC+ D 154 μm
Total	2.7 ± 0.4	3.7 ± 0.5
Reg 1	3.7 ± 0.7	2.7 ± 0.9
Reg 2	5.1 ± 0.8	7.6 ± 0.9
Reg 3	9.6 ± 1.6	6.8 ± 1.7

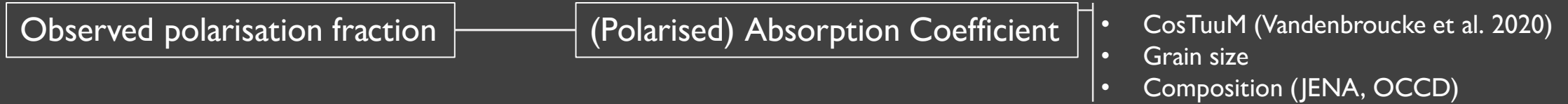
After synchrotron subtraction:

- p decreases in all regions at $154 \mu\text{m}$
- p decreases only in region 1 at $89 \mu\text{m}$ (-ish)

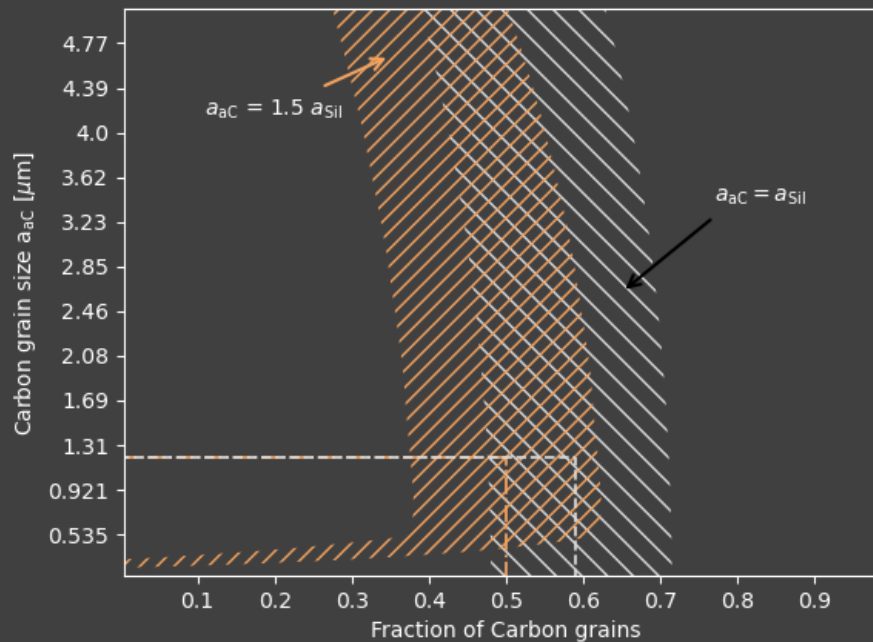
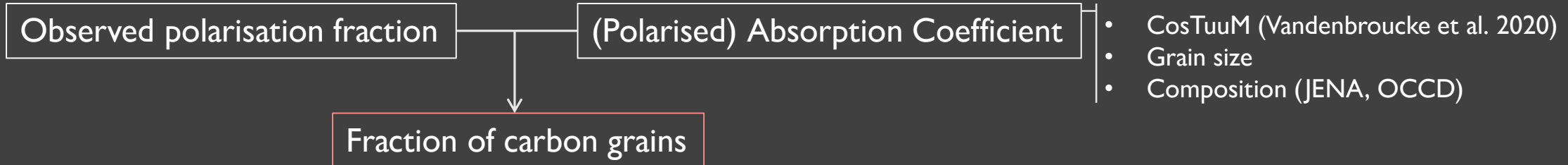
Between bands:

- regions 1 and 3 have lower p at $154 \mu\text{m}$
- region 2 has higher p at $154 \mu\text{m}$

HOW TO CONSTRAIN DUST PROPERTIES?

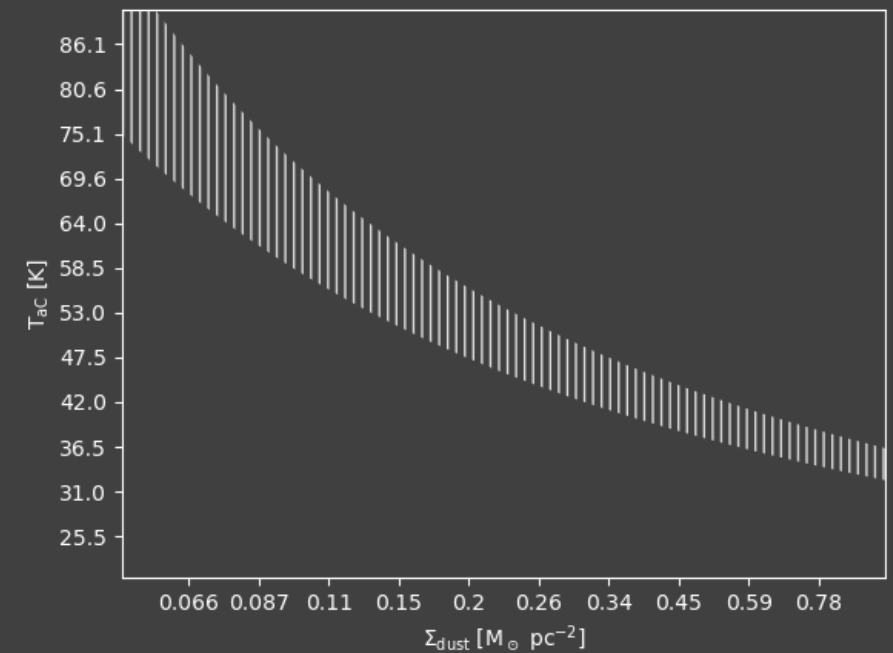
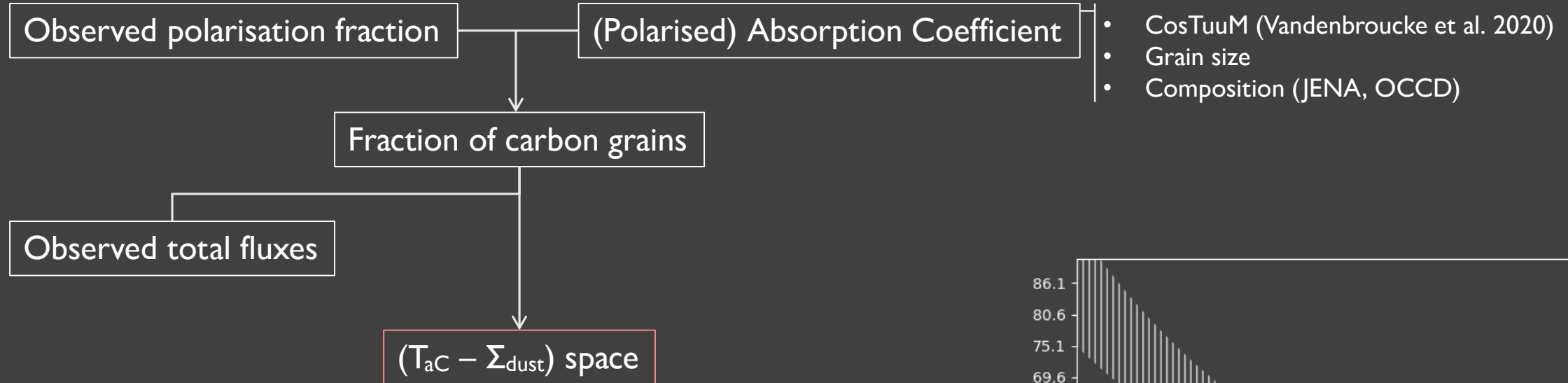


HOW TO CONSTRAIN DUST PROPERTIES?



$$p = \frac{(1 - f_{ac}) Q_{\text{abs, pol, Sil}}(\lambda, a)}{f_{ac} Q_{\text{abs, ac}}(\lambda, a) + (1 - f_{ac}) Q_{\text{abs, Sil}}(\lambda, a)}$$

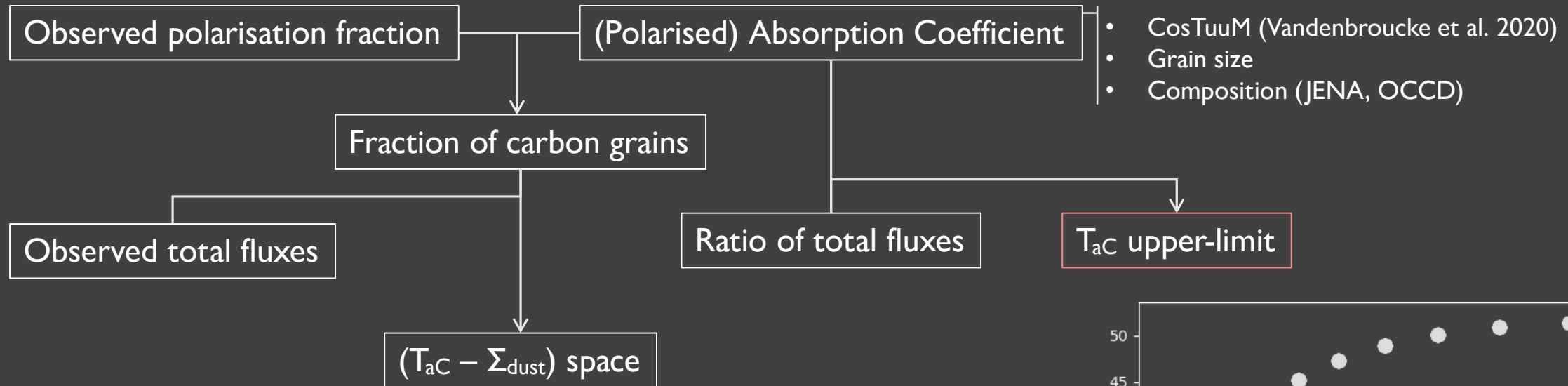
HOW TO CONSTRAIN DUST PROPERTIES?



$$S_{\nu, \text{tot}} = f_{aC} S_{\nu, aC} + (1 - f_{aC}) S_{\nu, \text{Sil}}$$

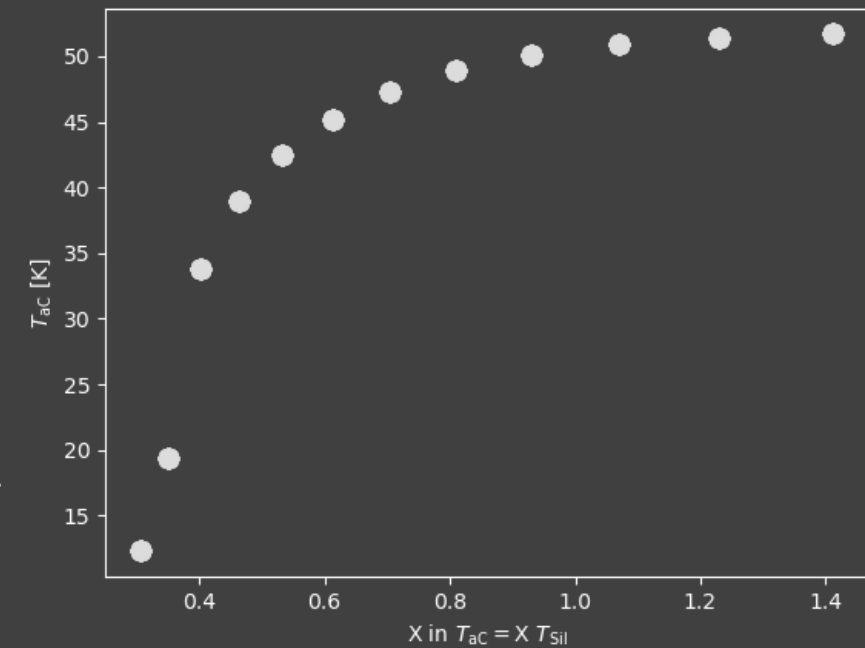
$$S_{\nu} = \kappa(\lambda, a) \Sigma_{\text{dust}} B(\lambda, T_{\text{dust}})$$

HOW TO CONSTRAIN DUST PROPERTIES?

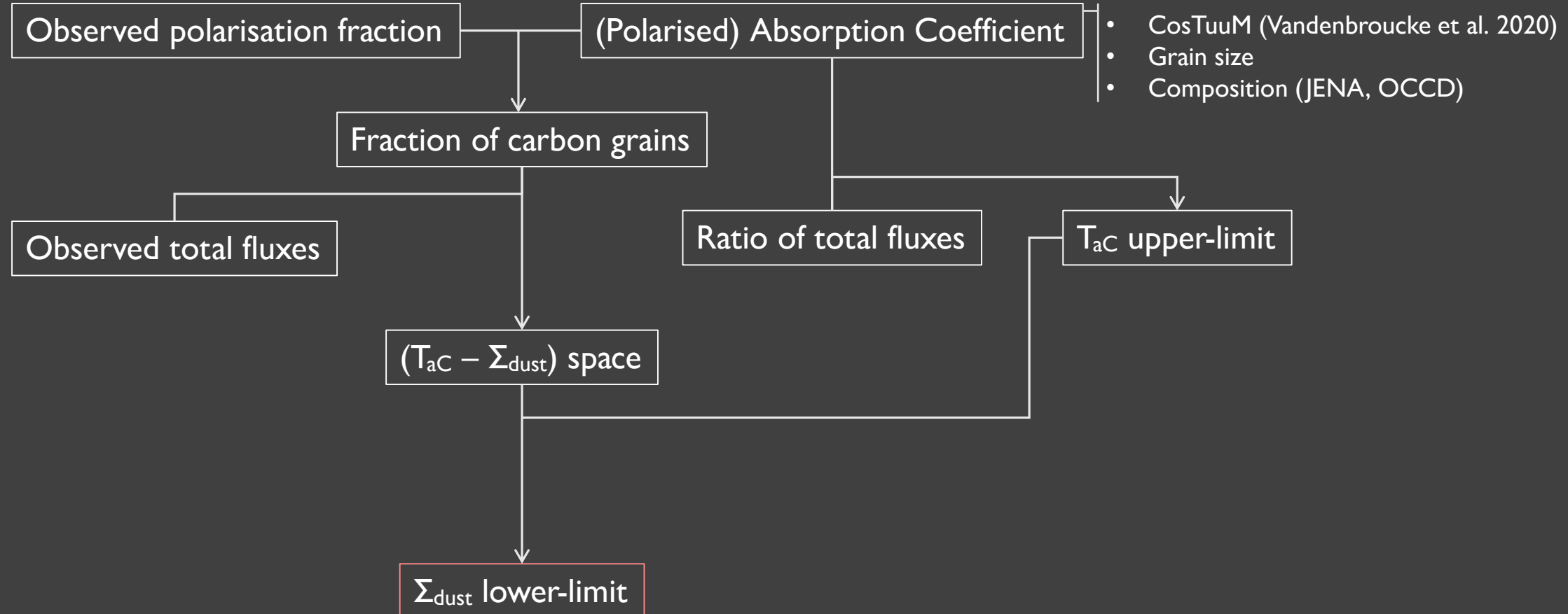


$$\frac{S_{\text{tot}, \lambda_1}}{S_{\text{tot}, \lambda_2}} = \frac{f_{\text{aC}} \kappa_{\text{aC}, \lambda_1} B_{\lambda_1}(T_{\text{aC}}) + (1 - f_{\text{aC}}) \kappa_{\text{Sil}, \lambda_1} B_{\lambda_1}(T_{\text{aC}}/X)}{f_{\text{aC}} \kappa_{\text{aC}, \lambda_2} B_{\lambda_2}(T_{\text{aC}}) + (1 - f_{\text{aC}}) \kappa_{\text{Sil}, \lambda_2} B_{\lambda_2}(T_{\text{aC}}/X)}$$

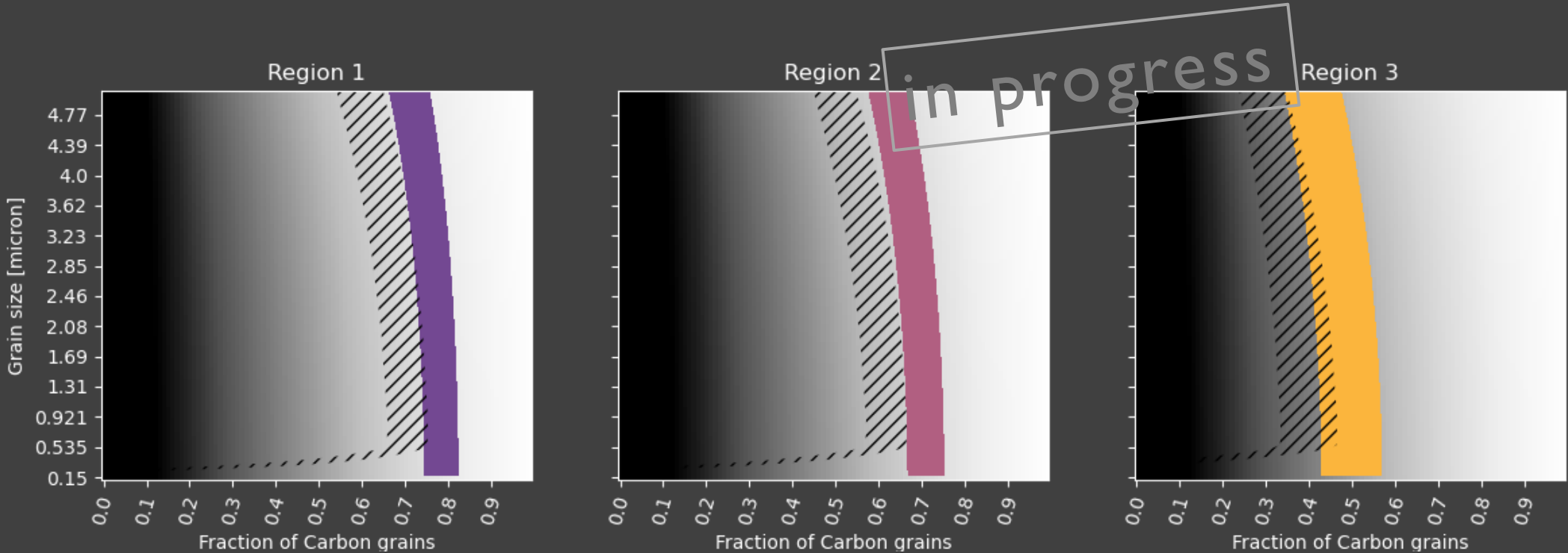
from Hankins et al. (2019)



HOW TO CONSTRAIN DUST PROPERTIES?



EXAMPLE: AC:H & MgSiO₃



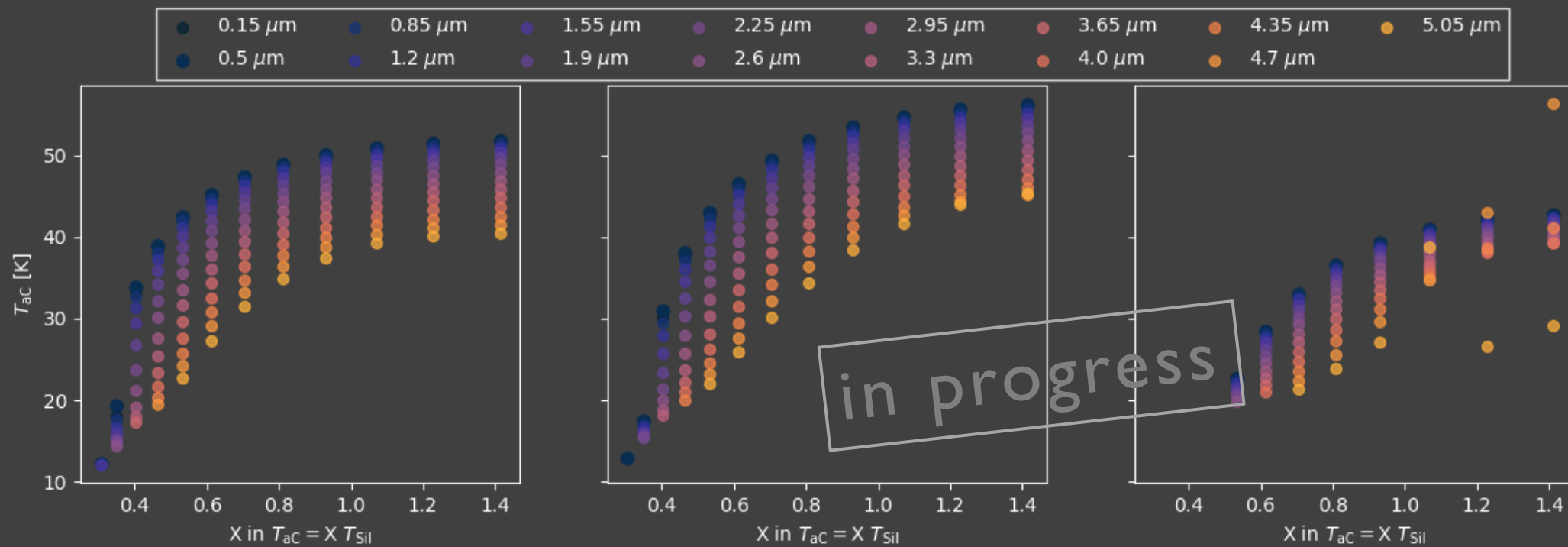
$$p = \frac{(1 - f_{ac}) Q_{\text{abs, pol, Sil}}(\lambda, a)}{f_{ac} Q_{\text{abs, ac}}(\lambda, a) + (1 - f_{ac}) Q_{\text{abs, Sil}}(\lambda, a)}$$

Refractive indices (n, k) and density

MgSiO₃: Jäger et al. (2003)

aC:H: optECs Eg = 0.1 eV (Jones et al. 2012)

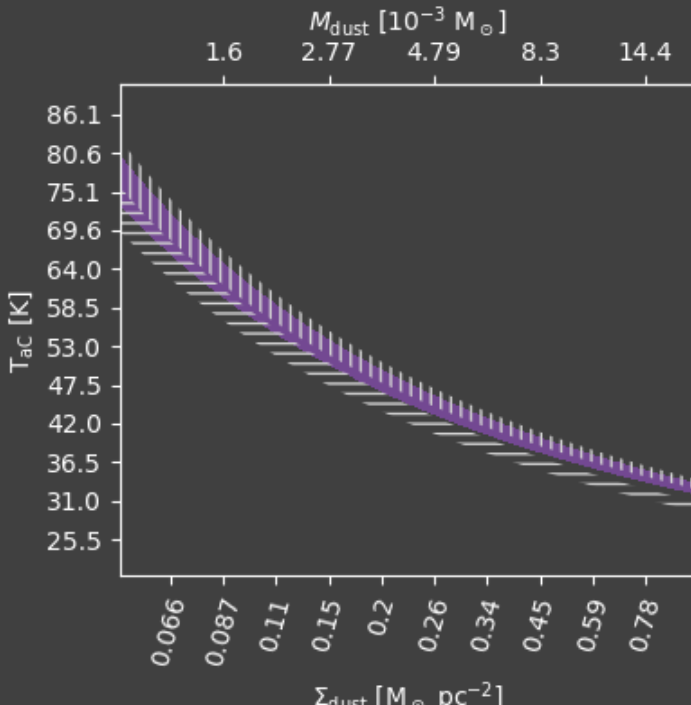
EXAMPLE: AC:H & MgSiO_3



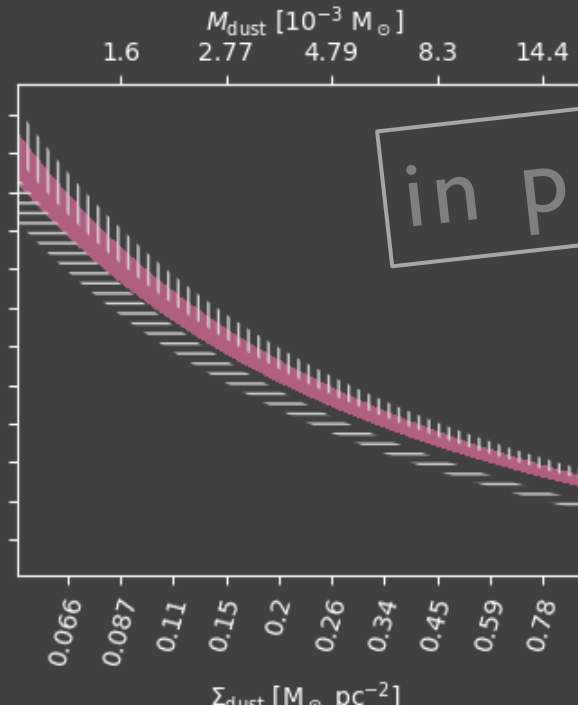
→ derive $T_{\text{ac}, \text{max}}$ in each region

$$\frac{S_{\text{tot}, \lambda_1}}{S_{\text{tot}, \lambda_2}} = \frac{f_{\text{ac}} \kappa_{\text{ac}, \lambda_1} B_{\lambda_1}(T_{\text{ac}}) + (1 - f_{\text{ac}}) \kappa_{\text{Sil}, \lambda_1} B_{\lambda_1}(T_{\text{ac}}/X)}{f_{\text{ac}} \kappa_{\text{ac}, \lambda_2} B_{\lambda_2}(T_{\text{ac}}) + (1 - f_{\text{ac}}) \kappa_{\text{Sil}, \lambda_2} B_{\lambda_2}(T_{\text{ac}}/X)}$$

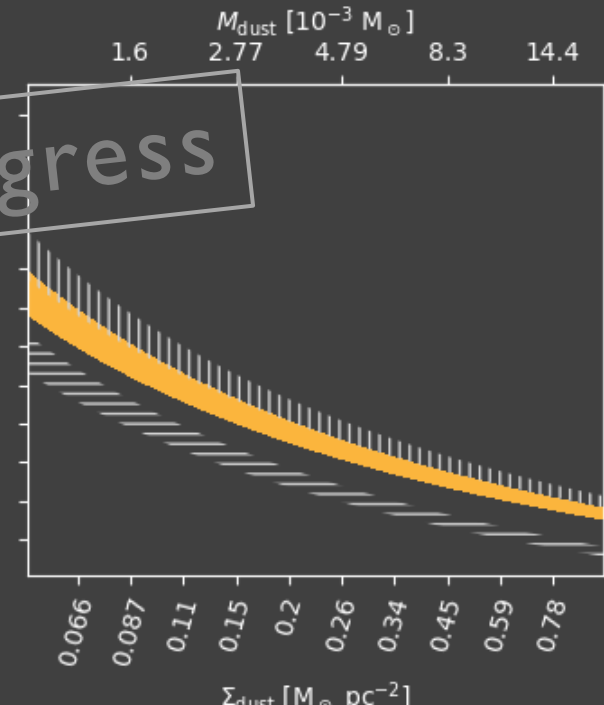
EXAMPLE: AC:H & MgSiO₃



$$M_{dust} \gtrsim 2.65_{0.24}^{0.27} \times 10^{-3} M_\odot$$



$$M_{dust} \gtrsim 2.31_{0.21}^{0.23} \times 10^{-3} M_\odot$$



$$M_{dust} \gtrsim 2.84_{0.37}^{0.41} \times 10^{-3} M_\odot$$

SO MANY VARIATIONS

- Composition:
 - $\text{Mg}_{0.5}\text{Fe}_{0.5}\text{SiO}_3 \rightarrow f_{aC}$ increases
 - $\text{MgFeSiO}_4 \rightarrow f_{aC}$ increases
 - $\text{Mg}_{0.7}\text{SiO}_{2.7} \rightarrow f_{aC}$ decreases

So MANY VARIATIONS

- Composition:
 - $\text{Mg}_{0.5}\text{Fe}_{0.5}\text{SiO}_3 \rightarrow f_{aC}$ increases
 - $\text{MgFeSiO}_4 \rightarrow f_{aC}$ increases
 - $\text{Mg}_{0.7}\text{SiO}_{2.7} \rightarrow f_{aC}$ decreases
- Size distributions:
 - Carbon and silicate grains unlikely to have same size
 - Include size distribution and non-polarising grains

SO MANY VARIATIONS

- Composition:
 - $\text{Mg}_{0.5}\text{Fe}_{0.5}\text{SiO}_3 \rightarrow f_{aC}$ increases
 - $\text{MgFeSiO}_4 \rightarrow f_{aC}$ increases
 - $\text{Mg}_{0.7}\text{SiO}_{2.7} \rightarrow f_{aC}$ decreases
- Size distributions:
 - Carbon and silicate grains unlikely to have same size
 - Include size distribution and non-polarising grains
- Shape distributions:
 - Oblate grains \rightarrow increases f_{aC}
 - Prolate grains \rightarrow decreases f_{aC}

SO MANY VARIATIONS

- Composition:
 - $\text{Mg}_{0.5}\text{Fe}_{0.5}\text{SiO}_3 \rightarrow f_{aC}$ increases
 - $\text{MgFeSiO}_4 \rightarrow f_{aC}$ increases
 - $\text{Mg}_{0.7}\text{SiO}_{2.7} \rightarrow f_{aC}$ decreases
- Size distributions:
 - Carbon and silicate grains unlikely to have same size
 - Include size distribution and non-polarising grains
- Shape distributions:
 - Oblate grains \rightarrow increases f_{aC}
 - Prolate grains \rightarrow decreases f_{aC}
- Alignment angle:
 - f_{aC} increases with the alignment angle

CONCLUSIONS



- Confirmed polarisation detection in the Crab Nebula, the second SNR after Cassiopeia A!
 - implies the existence of large grains ($a > 0.05 - 0.1 \mu\text{m}$)
 - synchrotron-free polarisation fractions range from 3.7 to 9.1% at $89 \mu\text{m}$ and from 2.7 to 7.6% at $154 \mu\text{m}$, in three dusty regions.
- We constrain and compute the fraction of carbon grains using the observed polarisation and computing the (polarised) absorption coefficients for a range of grain sizes (and composition).
- Combining polarisation fraction, total fluxes and making (a lot of) assumptions, we can derive lower-limits for the total dust masses in these regions
 - assuming optECs properties for aC grains and MgSiO₃ for Sil grains, with similar effective radii of $0.5 \mu\text{m}$, we find $\sim 2.3 - 3.1 \times 10^{-3} M_{\odot}$.



EXTRA – THE MODIFIED ASYMPTOTIC ESTIMATOR

- Normalized Stokes vectors:

$$q = Q/I \quad u = U/I$$

- Biased polarisation and polarisation angle:

$$p = \sqrt{q^2 + u^2} \quad \theta_p = 0.5 \arctan(u/q)$$

- Debiased polarisation and error:

$$p_{MAS} = p - b^2 \frac{1 - e^{-p^2/b^2}}{2p}$$

$$b^2 = \sigma_u^2 \cos^2(\theta_p) + \sigma_q^2 \sin^2(\theta_p)$$

$$\sigma_p^2 = \sigma_q^2 \cos^2(\theta_p) + \sigma_u^2 \sin^2(\theta_p)$$

EXTRA – SYNCHROTRON REMOVAL

- Interpolation of the (resolved) synchrotron radiation at 89 and 154 μm
- Synchrotron polarisation fraction and angle from NIKA 150 GHz

$$p_{\text{radio}}, \theta_{\text{radio}}$$

- Synchrotron Stokes vectors:

$$P_{\text{sync}} = p_{\text{radio}} I_{\text{sync}}$$

$$Q_{\text{sync}} = P_{\text{sync}} \cos(2 \theta_{\text{radio}})$$

$$U_{\text{sync}} = P_{\text{sync}} \sin(2 \theta_{\text{radio}})$$

- Synchrotron-free Stokes vectors:

$$I_{\text{final}} = I_{\text{HAWC}} - I_{\text{sync}}$$

$$Q_{\text{final}} = Q_{\text{HAWC}} - Q_{\text{sync}}$$

$$U_{\text{final}} = U_{\text{HAWC}} - U_{\text{sync}}$$

EXTRA – SYNCHROTRON MAPS

